15A
2d

OCT 7 1963

MASTER

CONF-299-1

BOEING

DOCUMENT NO. D2-90173

UNCLASSIFIED TITLE TRANSIENT RADIATION EFFECTS IN CAPACITORS AND DIELECTRIC MATERIALS

MODEL NO. RESEARCH CONTRACT NO.

ISSUE NO. 28 ISSUED TO Atomic Ener

Hicklin, H. W. et al.

SEATTLE, WASHINGTON

THE **BOEING** COMPANY

SEATTLE 24, WASHINGTON

DOCUMENT NO. D2-90173

UNCLASSIFIED TITLE TRANSIENT RADIATION EFFECTS IN CAPACITORS AND DIELECTRIC MATERIALS

MODEL NO. RESEARCH CONTRACT NO. ________

ISSUE NO. 28 ISSUED TO Atomic Energy Comm.

CLASSIFIED TITLE ________
(STATE CLASSIFICATION)

71335	2-5471	540010
WORK ORDER NO.	UNIT NO.	ITEM NO.

SPECIAL LIMITATIONS ON ASTIA DISTRIBUTION

ASTIA may distribute this report to requesting agencies subject to their security agreement, approved fields of interest, and the following:

X UNLIMITED - To all agencies of the Department of Defense and their contractors.

LIMITED - To U.S. Military organizations only.

This report may be distributed to nonmilitary agencies not approved above subject to BOEING approval of each request.

NOTE: The LIMITED category may be checked only because of actual or potential patent, proprietary, ethical, or similar implications.

PREPARED BY	H. W. Wicklein	4/25/62
PREPARED BY	R. H. Dickhaut	4/25/62
SUPERVISED BY	G. L. Keister	5/15/62
APPROVED BY	Edwin N York for W. B. Adam	5/15/62
CLASS. & DISTR. APPROVED BY	Edwin N York for W. B. Adam	5/15/62
		(DATE)

NO. OF PAGES 16 (EXCLUDING TITLE AND REVISION AND ADDITION PAGES.)

DOCUMENT TITLE PAGE

U3 4010 5000

PREFACE

This document contains a technical paper which resulted from work performed under U.S. Air Force contracts AF 04(647)-289, AF 33(616)-7531 and AF 33(616)-7804. The paper was presented at the IRE Western Electric Show and Convention in San Francisco, California, August 22-25, 1961.

TRANSIENT RADIATION EFFECTS IN CAPACITORS AND DIELECTRIC MATERIALS*

H. W. Wicklein and R. H. Dickhaut
The Boeing Company
Seattle, Washington

Measurements of dielectric leakage, capacitance, electric strength, and charge scattering phenomena have been performed at the Kukla and Godiva III critical assemblies for tantalum and aluminum electrolytic, wax- and oil-impregnated paper, mylar, mica, and ceramic capacitors, and for mylar and Vitamin Q-impregnated paper. Leakage data indicate that gamma-induced conductivity in capacitor dielectric varies directly with $\dot{\gamma}^{\Delta}$, where $\dot{\gamma}$ is the gamma radiation rate and Δ is 0.9 for mylar, 0.7 for Vitamin Q-impregnated paper, and approximately 1.0 for the other dielectrics. A small portion of the tantalum oxide conductivity induced by gamma radiation exhibits a recovery time of approximately 150 μs. Transient capacitance changes due to radiation are non-existent within $\pm$ 0.1 percent for mica and Vitamin Q capacitors. Transient charging of tantalum capacitors was noted during irradiation with no applied voltage. No drastic changes in electric strength were noted during irradiation of mylar and Vitamin Q-impregnated paper.

Results are compared with a summary of data collected by other investigators. The use of test data in parametric form as a tool for predicting transient radiation effects will be discussed.

Introduction

The effects caused in capacitors and dielectric materials by short, high-intensity bursts of nuclear radiation have been studied by various investigators for the past five years. An understanding of the nature and extent of these effects is essential in evaluating the vulnerability or reliability of various electronic circuits and systems when exposed to high-intensity radiation such as that from a nuclear weapon detonation.

High-intensity radiation causes ionization in materials due to scattering processes, photo effects, secondary emission, and other mechanisms. One would expect that the following capacitor properties, shown electrically in Figure 1, can be changed by the presence and distribution of the radiation-produced charge carriers caused by mechanisms mentioned above.

1. DC leakage--a change in shunt resistance (R_L) will be caused by increased conductivity in the dielectric material. Large conductivity changes are expected, in contrast to the usually low conductivity of dielectric materials in the absence of radiation.

2. Capacitance--a change in shunt capacitance (C_S) will be caused by changes in the effective dielectric constant of the dielectric material. Very small changes are predicted when the number of additional charge carriers due to radiation is considered.

3. Breakdown voltage--there is a possibility that a large increase in the number of conduction electrons can cause initiation of voltage breakdown at lower applied fields.

4. "EMF" generation--an apparent current source (i_{CH}) is possible due to differential scattering or secondary emission effects between dielectric and metal parts, and transport phenomena in the dielectric and electrolyte.

5. "Long-time" effects--trapping phenomena and the usually low conductivity of dielectric materials are conducive to the enhancement of conductivity with an associated time constant after the radiation burst. Trapped charges in the dielectric can cause polarization or persistence in the dielectric material so that subsequent radiation effects differ from the initial irradiation effect. Such effects are dose-dependent. In any radiation exposure there is a possibility of accumulating a sufficient radiation dose to cause permanent changes, but these permanent damage effects will not be considered in this paper. (The total doses received by test samples are not large enough to cause appreciable permanent effects in most capacitors and dielectric materials.)

The work at Boeing for the last year has been directed toward determining a quantitative description of the capacitor which can be used to predict circuit response to high-intensity radiation pulses. In performing this work use was made of existing pulse radiation data which were available on most of the capacitor properties mentioned above. In addition, extensive work was performed by Boeing in the measurement of DC leakage, capacitance changes, dielectric breakdown, and EMF generation. The results of this work, plus that of other investigators, has resulted in a successful circuit representation of the capacitor.

Experimental Studies

Radiation Source

Tests have been performed at the Godiva III (Los Alamos Scientific Laboratories) and Kukla (Lawrence Radiation Laboratory) pulse reactors. The two facilities provide similar mixed neutron-gamma radiation pulses of the shape shown in Figure 2. Average peak gamma rates up to 5×10^7 r/sec are obtained and average pulse widths at half-intensity range from 65 to 300 μs. Total radiation doses of 5000 r and 1×10^{13} neutrons/cm^2 (energy > 4 Kev) are obtained. The gamma and neutron energies are equivalent to a fission spectrum.

Instrumentation

DC leakage measurements were performed with the circuit shown in Figure 3.

AC capacitance measurements were performed by using constant-current and constant-voltage circuits to measure changes in capacitive reactance at 50 kc. The maximum sensitivity for these measurements is ± 0.5 percent when a magnified oscilloscope trace amplitude is used. However, the most accurate measurements of capacitance were performed with the resonant circuit shown in Figure 3. Inductance values in the range 10 to 1000 μhy were used at test frequencies from 50 to 150 kc. The circuit was tuned slightly off resonance prior to each test. Capacitance changes of ± 0.1 percent could be detected.

A special test fixture, shown in Figure 4, was designed to measure electric strength with >4000 V applied and to measure conductivity in thin (1-5 mil) samples of dielectric materials. The fixture was used in place of the capacitor in the leakage test circuit. The electrodes are 0.25 inches thick with rounded edges and parallel within ± 0.0001 inch. The micrometer allows adjustment for sample thickness to within ± 0.0001 inch. The high voltage (removable) electrode is 1.0 inch diameter and rides on a needle point; it is surrounded by a nylon ring to reduce surface breakdown and air ionization effects. The dielectric test samples extended at least 0.25 inch past the edges of the 1.5 inch diameter low voltage electrode. Air ionization effects are reduced by the long conduction path compared with the dielectric thickness, and by the current flow from high-voltage electrode to the grounded frame rather than to the low-voltage electrode. The circuit connections were made so that only the current from the low-voltage electrode was measured.

All data were transmitted over coaxial cables to high-gain oscilloscope channels with photographic recording, and the cables were terminated in their characteristic impedance (R_T). The shunt capacitance from the battery to ground does not create a problem for the pulse frequencies involved. Capacitor sample electrical connections were potted to reduce air ionization effects.

Dosimetry

Gamma rates were determined from the correlation of pulse shape data with the total gamma dose received by chemical dosimeters (± 10.0 percent accuracy). The assumption has been that all the dose recorded by the chemical dosimeters is due to gamma radiation, but this has not been proven as yet. All dosimeters were mounted next to the test specimens.

Data and Analysis

The results of the capacitance change experiment indicate that there are no changes in capacitance within the measurement accuracy of the test equipment. The actual lower limit for the capacitors measured are ± 0.1 percent for Vitamin Q and silver mica capacitors at a gamma rate of 1.0×10^7 r/sec, ± 0.5 percent for tantalum solid capacitor at 3×10^7 r/sec, ± 1.0 percent for oil-impregnated paper, (polarized) and (non-polarized) tantalum foil capacitors at 1×10^6 and 4.0×10^7 r/sec respectively, and ± 15.0 percent for mylar capacitors at 2.0×10^6 r/sec.

A voltage breakdown test on 6×10^{-3} cm thickness of Vitamin-Q-impregnated paper indicated that a radiation rate of 1×10^6 r/sec would not induce breakdown when the voltage was within 25 percent of the normal breakdown voltage.

A significant EMF generation signal was obtained only for polarized electrolytic capacitors.

EMF generation data were taken for tantalum solid, (polarized and non-polarized) plain foil and etched foil tantalum, and etched foil aluminum capacitors. Sample data are shown in Figure 5 as a function of gamma dose and time. The non-polarized capacitor (data not shown) showed a very small effect compared with the polarized capacitors. The EMF generation data are not sufficiently accurate for detailed analysis; however, it is indicated that an integrated effect occurs during rapid dose accumulation to the pulse peak, and that a time decay effect occurs during the time following the peak. A possible explanation is that the charge carriers scattered onto the anode are collected immediately, but that the charge carriers scattered into the electrolyte cathode require a time longer than the time to the pulse peak for the electrons to diffuse in the electrolyte and for the dissociation or equilibrium state of the electrolyte to return to normal. This mechanism would account for the observed signals, including the lack of signal in the non-polarized capacitor. EMF generation should not appear in non-electrolytic capacitors. A test on one uncharged 1.0 µf Vitamin Q capacitor showed no signal within ± 0.1 mv. EMF generation effects would not appear when voltage is applied to enhance diffusion of scattered electrons in the cathode of the electrolytic capacitors.

The major effect in capacitors is the reduction in leakage resistance due to the increase in the dielectric conductivity. The most extensive measurements have been made on capacitor DC leakage and dielectric conductivity.

DC leakage tests were performed on mylar, Vitamin-Q-impregnated paper, and samples of Silastic RTV 881 potting compound. DC leakage tests were made on ceramic, oil-impregnated paper, wax-impregnated paper, oil bath, silver mica, Vitamin Q, tantalum solid, tantalum foil, and aluminum foil capacitors in the range from .01 to 15,000 µf. Sample capacitor leakage data are shown in Figure 6. In general, smaller values of capacitance yield signals which approximate the radiation pulse. Larger capacitors yield signals which do not exhibit recovery during the duration of the burst, and have a time decay constant markedly different from the radiation pulse shape. This is due to the measurement circuit time constant.

Leakage data taken with the dielectric test fixture were converted to conductivity by using the parallel plate relationships with the known fixture geometry and dielectric thicknesses. Capacitor data were converted to leakage resistance by using the dynamic circuit equation given in Figure 6. These leakage resistance values were then converted to conductivity values for the dielectric materials by using parallel plate assumptions (for thin dielectrics) and the values of capacitance and dielectric constant for the specific capacitor.

In cases where the coaxial transmission cable signal is the same order of magnitude as the observed signal, a correction must be made. The cable signal must be subtracted from the observed signal in order to obtain the true capacitor signal as shown in Figure 7. It is obvious from Figure 7 that a sizeable cable signal can change not only the amplitude, but also the time dependence of the signal.

It is found that gamma induced conductivity in dielectric materials follows the relationship

$$\sigma = K\dot{Y}^{\Delta} \qquad (1)$$

where $\dot{Y}$ is gamma rate and Δ is 0.7 for Vitamin Q-impregnated paper, 0.9 for mylar, and approximately 1.0 for the other materials tested. This relationship is only approximate to the peak of the radiation burst for tantalum-oxide and the oil-bath capacitor (Dykanol G oil-impregnated paper). These materials do not show immediate recovery after the radiation pulse. An example of this long time effect is shown in Figure 8 for Ta_2O_5. The conductivity in the oil bath capacitor exhibited an exponential time decay with a time constant of 40-45 ms.

An empirical relationship was developed for the Ta_2O_5 capacitor using experimental data similar to that shown in Figure 8. The conductivity was separated into two parts: σ_1 is proportional to the gamma rate; σ_2 is proportional to the total dose and a decay factor which is long compared with the duration of the burst. A typical separation of this type is shown in Figure 9. Figure 10 shows the empirical relationship. Several of the more accurate data were solved simultaneously to determine the time decay constant (τ_1) for σ_2 (assuming σ_1 negligible at long times). Then σ_2 was reconstructed throughout a typical pulse by iteration. Dose proportionality constants (k_2) for σ_2 were found by matching the reconstructed curve to the long time portions of the data. The rate constants (K_1) were then found for σ_1 by subtracting σ_2, and taking the slope of the σ_1 versus $\dot{Y}$ curve. A summary of the empirically determined constants appears in Figure 10. The rate and dose constants are different for solid and foil type capacitors, apparently due to the nature of the electrolyte. There were no significant differences between polarized and non-polarized, or plain and etched foil types.

None of the capacitor data indicated dependence of gamma induced conductivity on applied electric field, dielectric thickness, or capacitance value.

Summary of Data

The experimental results for capacitance and leakage are consistent with data taken by other investigators such as International Business Machines Corp., Diamond Ordnance Fuze Laboratory, and Sandia Corp. Figure 11 shows a summary of DC leakage data in terms of conductivity as a function of gamma rate. IBM data have been converted as closely as possible to this representation. The data for Ta_2O_5 capacitors includes only σ_1. The dose dependent portion σ_2 is necessary after the radiation peak.

Applications

The data for transient radiation effects in capacitors and dielectric materials can be used to predict transient radiation effects in electronic circuits and systems. The equivalent circuit for an irradiated capacitor is shown in Figure 12. C_S is $< \pm 0.001C$ and i_{CH} is negligible when voltage is applied. R_L can be calculated from the equation for parallel plate approximation given in Figure 12, where $\sigma = \sigma_1 + \sigma_2$ is the measured dependence on gamma dose and rate. The resulting equivalent circuit can be substituted in the circuit of interest in place of the capacitors, and the transient effect on the circuit can be calculated by an analog computer when the appropriate gamma dose and gamma rate environment are provided.

* Work supported by U. S. Air Force contracts AF 04(647)-289, AF 33(616)-7531, and AF 33(616)-7804. Contract AF 33(616)-7804 sponsored by Advanced Research Projects Agency, Department of Defense.

① EQUIVALENT CIRCUIT FOR CAPACITOR DURING IRRADIATION

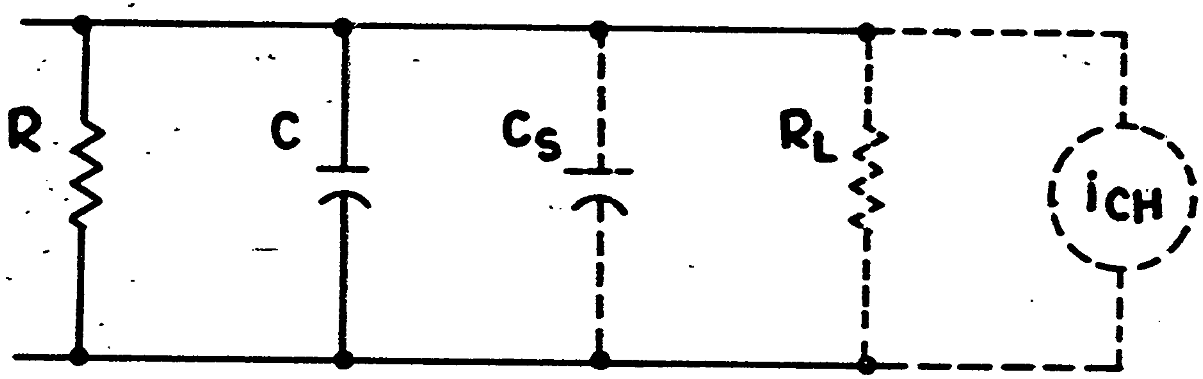

② TYPICAL GODIVA III RADIATION PULSE

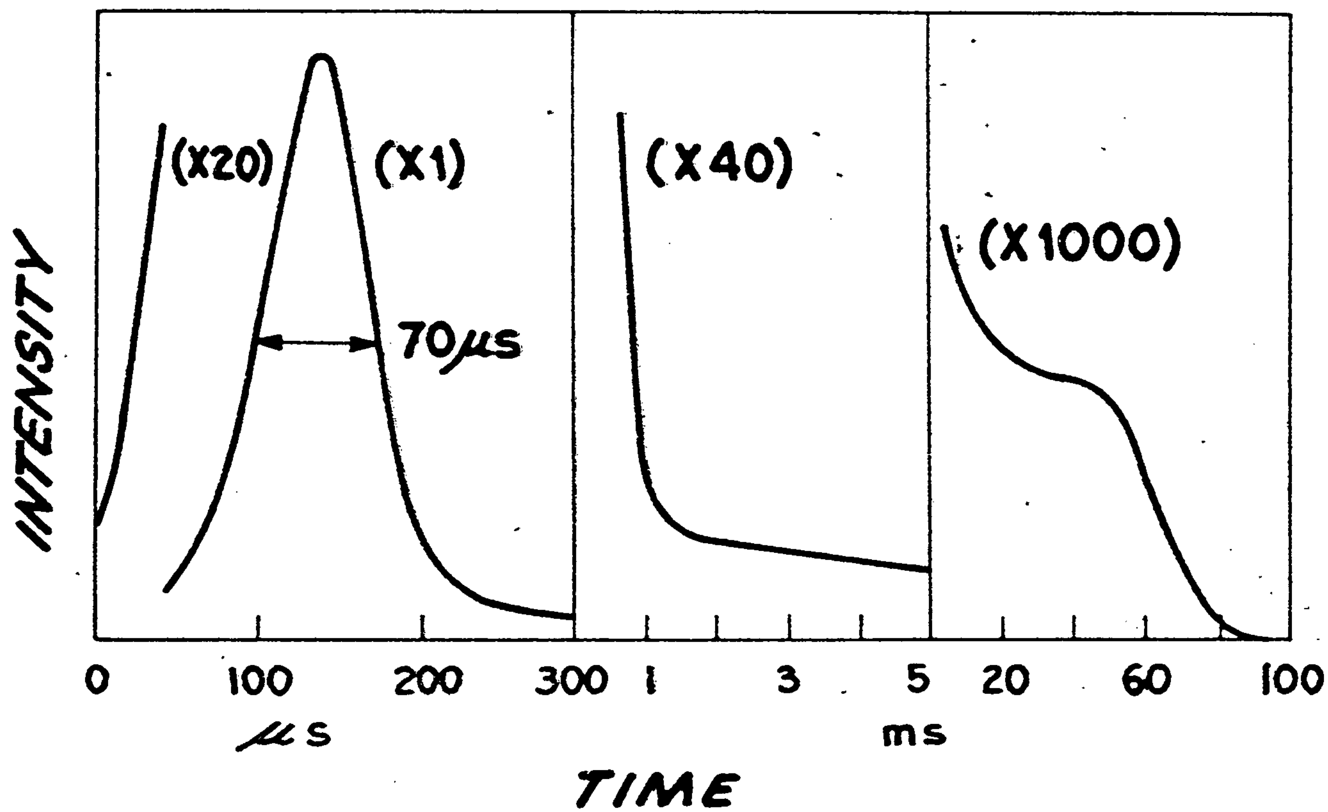

③ D.C. LEAKAGE TEST CIRCUIT

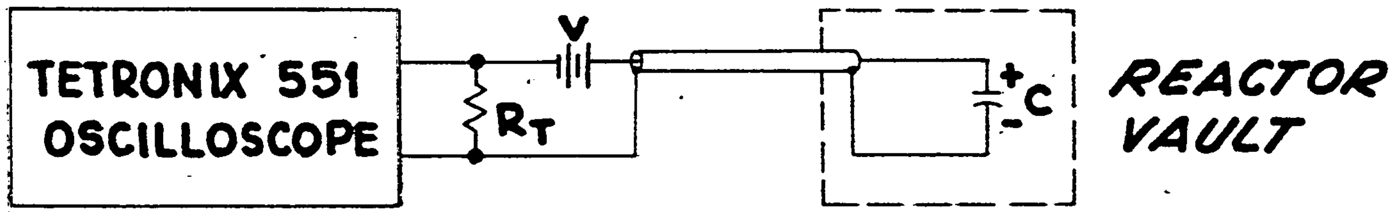

A.C. CAPACITANCE TEST CIRCUIT

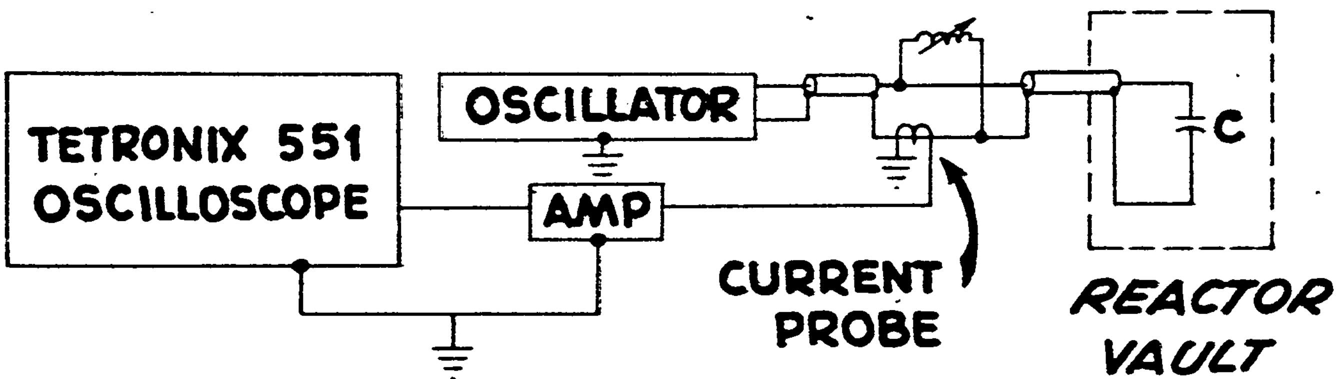

4 DIELECTRIC TEST FIXTURE

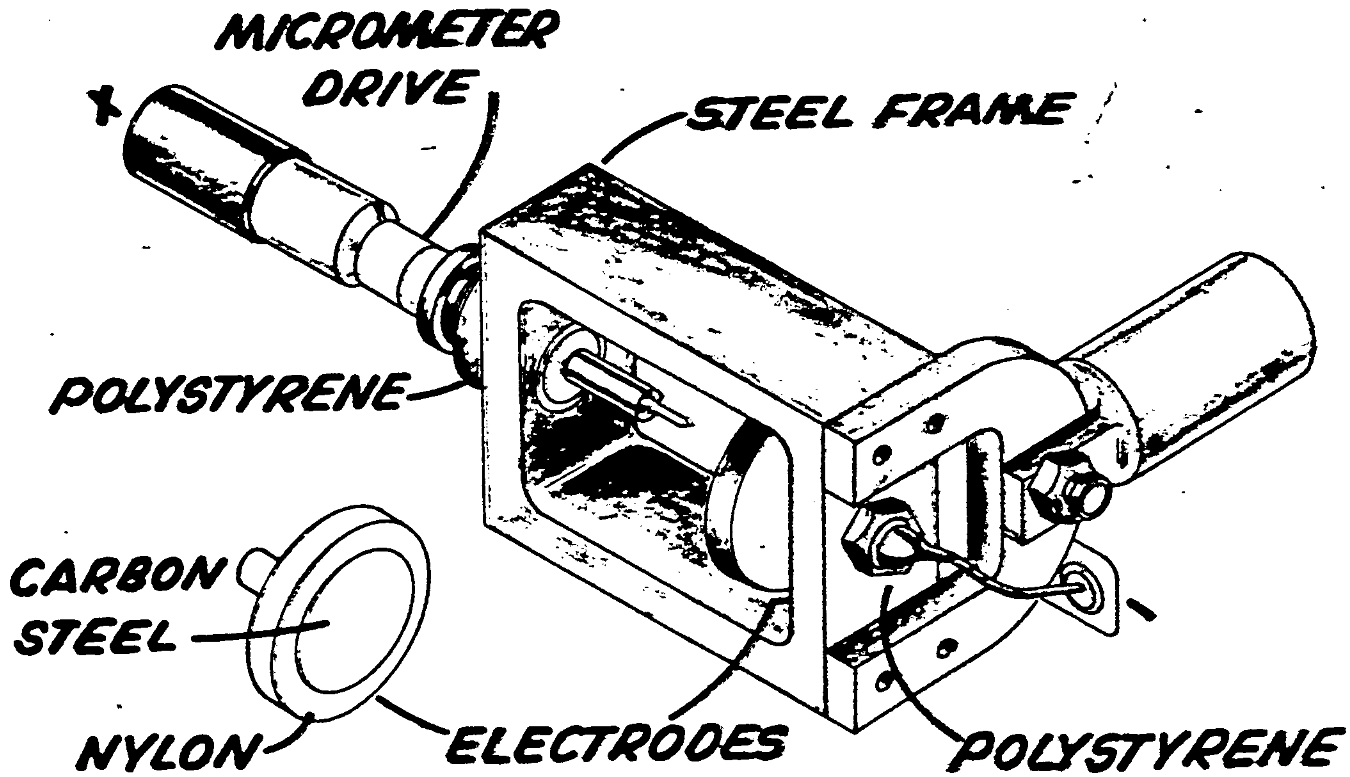

5 EXPERIMENTAL DATA FOR UNCHARGED ELECTROLYTIC CAPACITORS

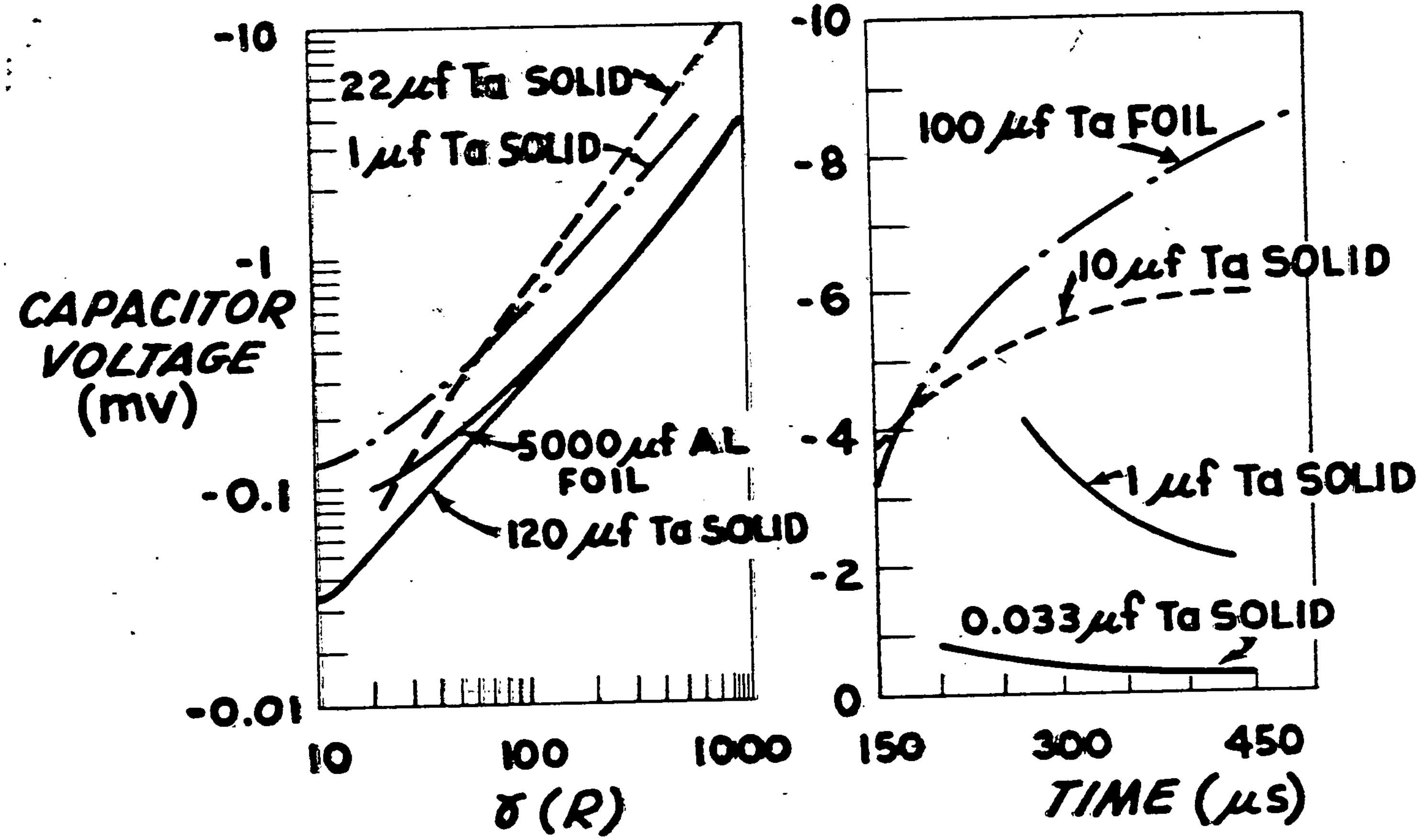

6 DC LEAKAGE DATA FOR 3 μf Ta FOIL CAPACITOR

$$R_L = \frac{(V - v) R_T}{v - R_T C \frac{dv}{dt}}$$

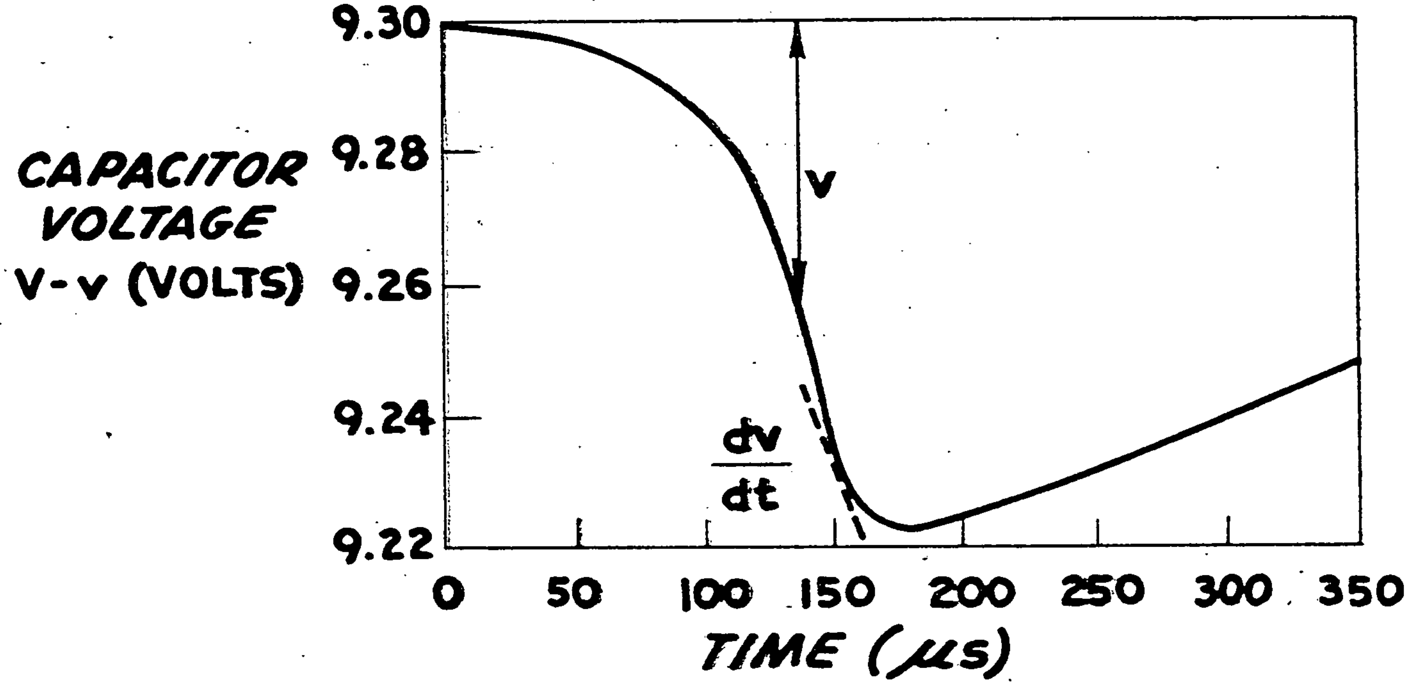

7 TYPICAL CABLE EFFECT ON CAPACITOR LEAKAGE SIGNAL

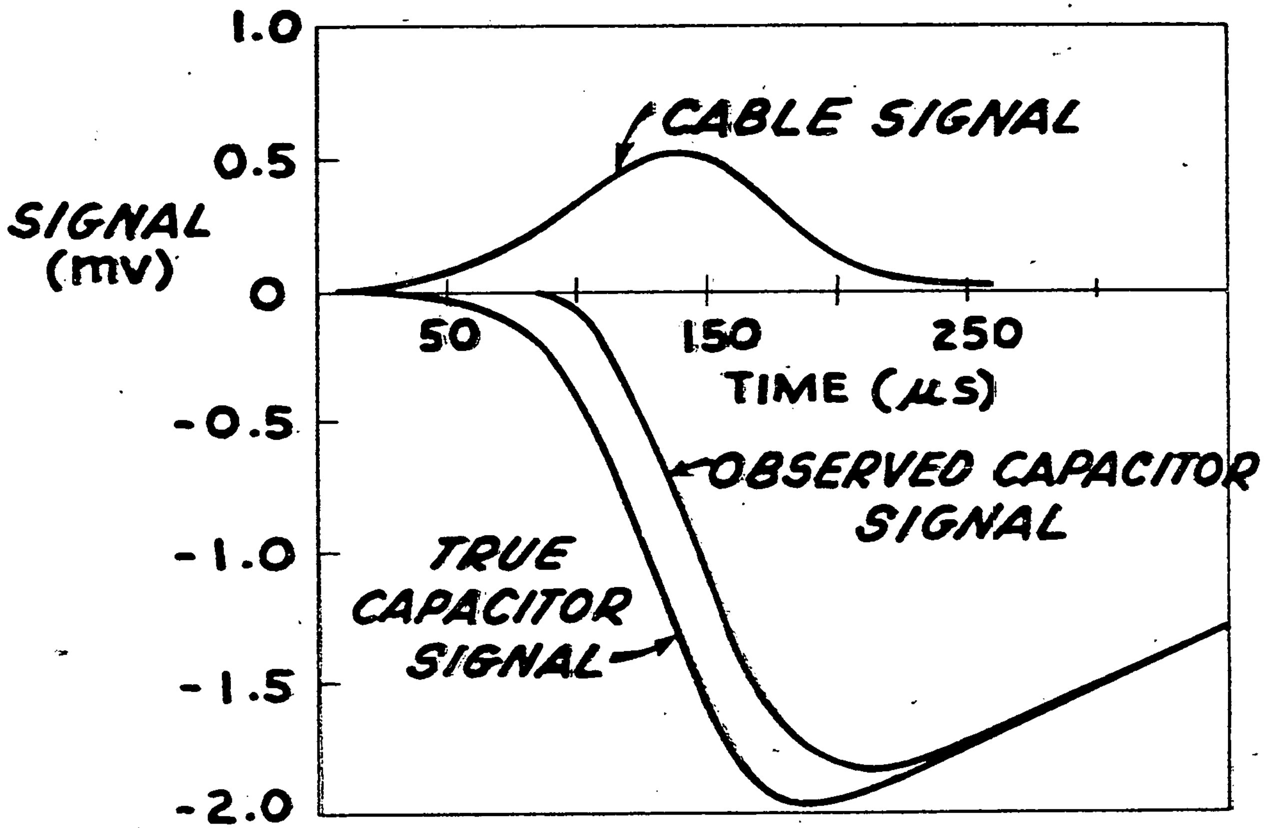

8 CONDUCTIVITY & GAMMA RATE PULSES FOR 3μf Ta FOIL CAPACITOR

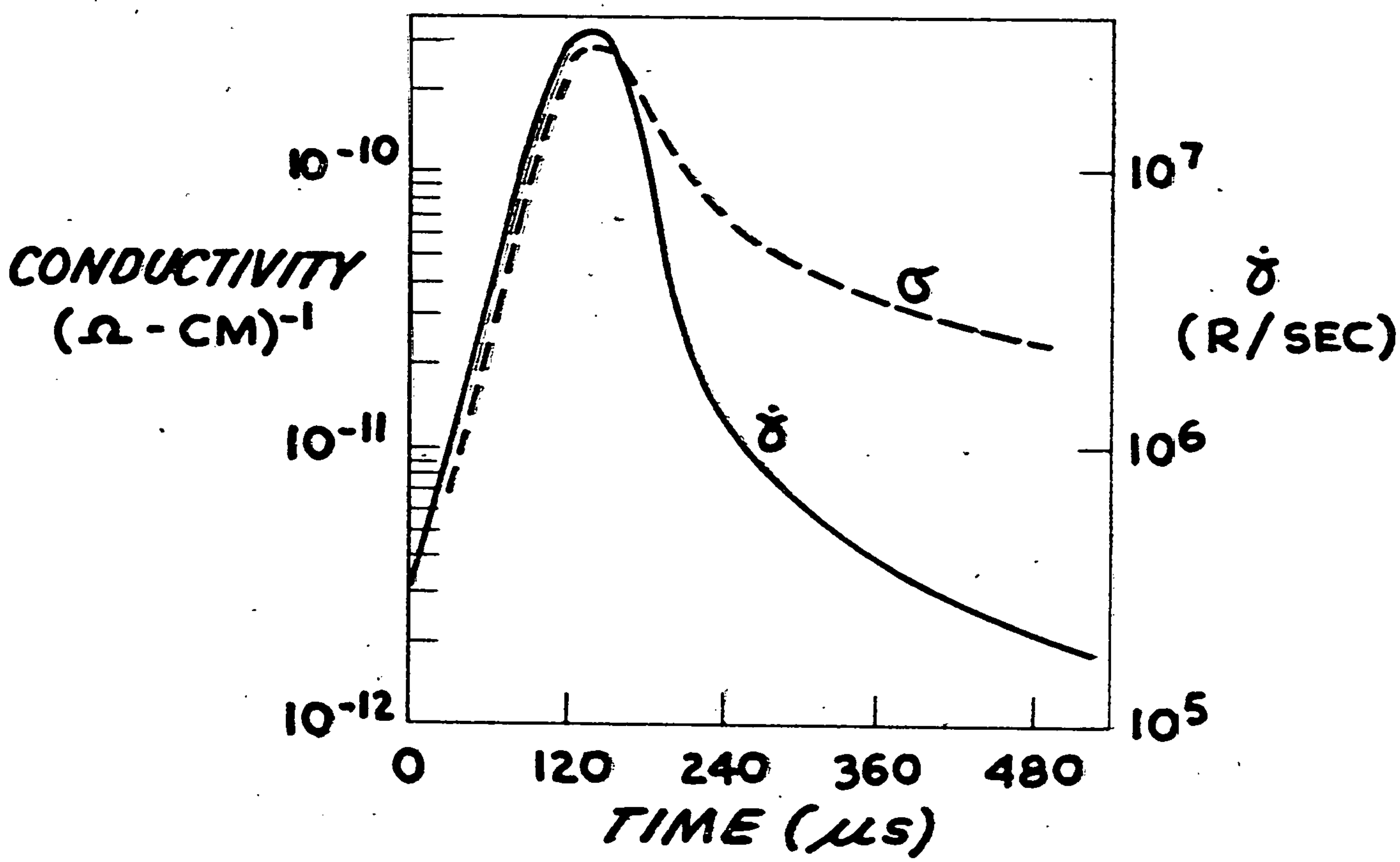

9 CONDUCTIVITY ANALYSIS FOR 3 μf Ta FOIL CAPACITOR

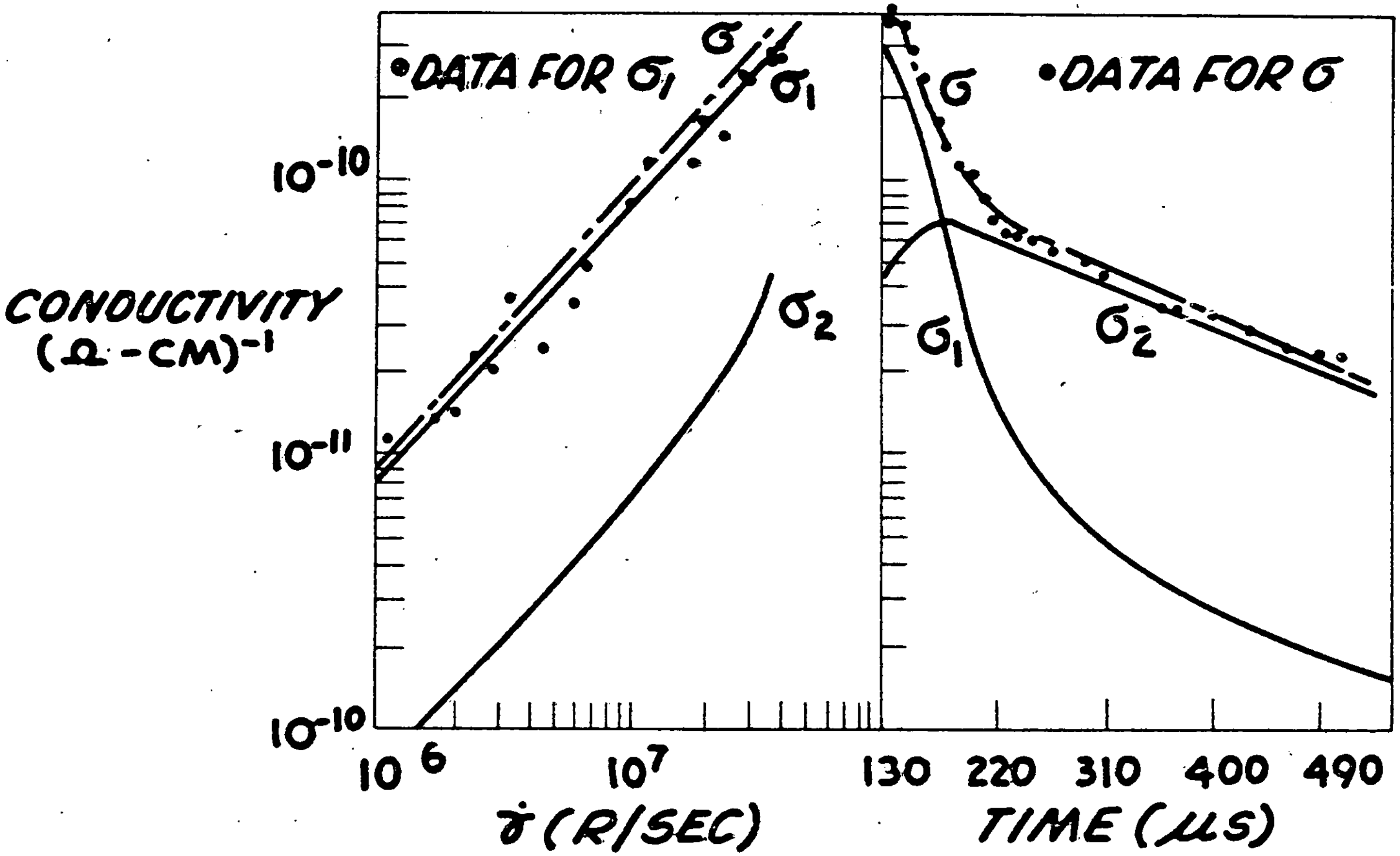

(10) RESULTS OF Ta_2O_5 CONDUCTIVITY ANALYSIS

$$\sigma = \sigma_1 + \sigma_2$$

$$\sigma_1 = K_1 \dot{\gamma}$$

$$\sigma_2 = K_2 \gamma_t - \int_0^t \frac{\sigma_2}{\tau_2}\, dt$$

$$\tau_2 = 2.18 \times 10^{-4} \text{ sec}$$

	FOIL TYPES (9)	*SOLID ELECTROLYTE (3)*
K_1 $\frac{\text{sec}}{(\Omega\text{-cm})r}$	$6.7^{+4.1}_{-2.9} \times 10^{-18}$	$12.2^{+2.9}_{-2.6} \times 10^{-18}$
K_2 $\left[(\Omega\text{-cm})r\right]^{-1}$	$1.8^{+1.6}_{-1.2} \times 10^{-14}$	$7.2^{+2.6}_{-4.3} \times 10^{-14}$

(11) SUMMARY OF DC CONDUCTIVITY DATA - BOEING & IBM

$$\sigma_1 = K\dot{\gamma}^{\Delta}$$

DIELECTRIC	K	K	Δ
MYLAR	3	4.2×10^{-17}	0.9
VITAMIN Q IMPREG. PAPER	11	5.2×10^{-15}	0.7
TANTALUM OXIDE (APPROX.)	25	1.2×10^{-17}	1.0
ALUMINUM OXIDE	7	2.95×10^{-18}	1.0
GLASS	~6.5	2.0×10^{-17}	1.0 EST
OIL IMPREGNATED PAPER	~7	7.4×10^{-17}	~1.0
TEFLON	2	4.2×10^{-18}	~1.0
SILASTIC + DC - 200	-	$\sim 5.1 \times 10^{-15}$	~1.0
MICA	6.8	$\sim 1.0 \times 10^{-17}$	1.0 EST
CERAMIC	~20	$\sim 4.0 \times 10^{-17}$	1.0 "

12 EQUIVALENT CIRCUIT FOR CAPACITOR DURING IRRADIATION

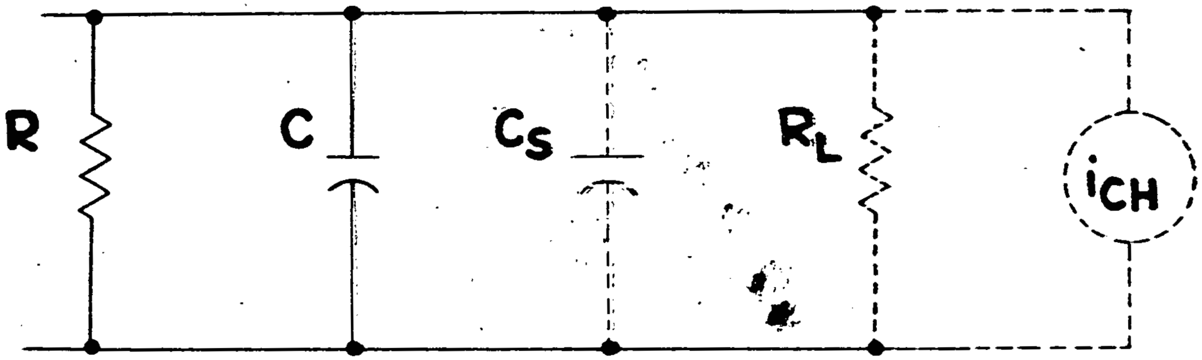

$$R_L = \frac{K\epsilon_0}{\sigma C} \qquad \sigma = \sigma_1 + \sigma_2$$

$C_S < .001C$

i_{CH} SMALL